Comparative Study of Tyrosine Radicals in Hemoglobin and Myoglobins Treated with Hydrogen Peroxide

Dimitri A. Svistunenko,* Jacqueline Dunne,* Michael Fryer,* Peter Nicholls,* Brandon J. Reeder,* Michael T. Wilson,* Maria Giulia Bigotti,† Francesca Cutruzzolà,† and Chris E. Cooper*

*Department of Biological Sciences, Central Campus, University of Essex, Colchester CO4 3SQ, United Kingdom; and †Department of Biochemistry, University of Rome La Sapienza, 00185 Rome, Italy

ABSTRACT The reactions of hydrogen peroxide with human methemoglobin, sperm whale metmyoglobin, and horse heart metmyoglobin were studied by electron paramagnetic resonance (EPR) spectroscopy at 10 K and room temperature. The singlet EPR signal, one of the three signals seen in these systems at 10 K, is characterized by a poorly resolved, but still detectable, hyperfine structure that can be used to assign it to a tyrosyl radical. The singlet is detectable as a quintet at room temperature in methemoglobin with identical spectral features to those of the well characterized tyrosyl radical in photosystem II. Hyperfine splitting constants found for Tyr radicals were used to find the rotation angle of the phenoxyl group. Analysis of these angles in the crystal structures suggests that the radical resides on Tyr151 in sperm whale myoglobin, Tyr133 in soybean leghemoglobin, and either αTyr42, βTyr35, or βTyr130 in hemoglobin. In the sperm whale metmyoglobin Tyr103Phe mutant, there is no detectable tyrosyl radical present. Yet the rotation angle of Tyr103 (134°) is too large to account for the observed EPR spectrum in the wild type. Tyr103 is the closest to the heme. We suggest that Tyr103 is the initial site of the radical, which then rapidly migrates to Tyr151.

INTRODUCTION

Electron paramagnetic resonance (EPR) spectroscopy reveals the presence of a free radical in frozen samples of blood (Chernov et al., 1994; Pulatova et al., 1989). This is similar to many other biological tissues. The free radicals in most tissues originate from the mitochondrial electron transport chain (Burgova et al., 1989; Vithayathil et al., 1965). However, there are few mitochondria in blood, so the presence of free radicals there needs a different explanation. We have shown instead that the free radical in blood originates from the reaction of methemoglobin (metHb) with hydrogen peroxide (Svistunenko et al., 1997b). The formation of this species in normal blood, in concentrations ranging from 0.5 to 2 μM, can be used to estimate the intensity of hemoglobin autoxidation in vivo (Svistunenko et al., 1997a,b). However, the chemical nature of the radicals in blood has not been unequivocally established because the EPR spectrum of the blood free radicals is an essentially featureless singlet, making the spectral assignment difficult.

When hemoglobin (Hb) or myoglobin (Mb) in the met form (i.e., in the Fe^{III} heme state) reacts with H_2O_2 or with other peroxides, the heme is oxidized to the (oxo)ferryl state Fe^{IV}═O. This one electron oxidation takes place along with H_2O_2 reduction to water, the latter being a two-electron process. The second electron, participating in H_2O_2 reduction, comes from the protein's globin, leaving it in the free radical state (Gibson and Ingram, 1956; Gibson et al., 1958; Kelso King et al., 1967; Kelso King and Winfield, 1963):

$$\underbrace{Fe^{III}\ R}\ + H_2O_2 \rightarrow \underbrace{Fe^{IV} = O\dot{R}^{+}} + H_2O \qquad (1)$$

Numerous studies have shown that the optically detectable $Fe^{III} \rightarrow Fe^{IV}$ transition is accompanied by a radical formation demonstrable by EPR spectroscopy. However, the nature and concentration of the radicals formed seem to be strongly dependent on the heme protein being studied. We have shown recently that both peroxyl ($ROO^{\bullet}$) and nonperoxyl radicals are formed in horse heart (HH) metMb, sperm whale (SW) metMb, and human metHb (metHbA) under H_2O_2 treatment and that the yield of these radicals is very different in the different proteins (Svistunenko, 2001).

The peroxyl radical in the HH metMb/H_2O_2 and SW metMb/H_2O_2 systems has been proven to originate from a tryptophan residue (DeGray et al., 1997; Gunther et al., 1995), identified as Trp14 in the case of SW Mb (DeGray et al., 1997). The location of the nonperoxyl radicals is less certain. In low-temperature EPR spectra this radical appears as a singlet (identical to the singlet in blood). The assignment of the singlet to a particular molecular structure is difficult because of the absence of any hyperfine structure or g-factor anisotropy. Comparisons with radicals generated from purified amino acids were equivocal, suggesting that phenylalanine, histidine, or tyrosine could all contribute to the observed spectrum (Kelso King et al., 1967).

Room-temperature studies have the ability to reveal a better resolved structure in EPR spectra. Surprisingly, the reactions of HH metMb and SW metMb with ethyl hydroperoxide (EtOOH) result in two different EPR spectra in the liquid phase: a five-component spectrum in SW metMb and a seven-component signal dominating the spectrum of

Submitted March 22, 2002, and accepted for publication June 20, 2002.

Address reprint requests to Dr Dimitri Svistunenko, Department of Biological Sciences, Central Campus, University of Essex, Wivenhoe Park, Colchester, Essex CO4 3SQ, UK. Tel.: 44-1206-873149; Fax: 44-1206-872592; E-mail: svist@essex.ac.uk.

0006-3495/02/11/2845/11 $2.00

HH metMb (Miki et al., 1989). The five-component spectrum was assigned to a tyrosyl phenoxyl radical in SW Mb, possibly Tyr151 (Miki et al., 1989). A similar five-component spectrum in leghemoglobin (Lb) treated with peroxides was tentatively assigned to the Tyr132 radical (Davies and Puppo, 1992).

In the case of Hb, the first direct observation of the radical in the metHb/H_2O_2 liquid-phase system was by Shiga and Imaizumi (1975). Although unable to identify the radical precisely because of lack of resolution in the hyperfine structure, the authors pointed out that it must involve a protein in a "slowly tumbling" situation. McArthur and Davies (1993) assigned a similar, also poorly resolved, spectrum in the metHb/peroxide system to a tyrosine-derived phenoxyl radical, stressing that the signal "bears considerable resemblance to those detected with a number of different types of myoglobin and leghemoglobin". However, as indicated above, the room-temperature spectra of the radicals are different in HH and SW myoglobins, making such comparisons ambiguous. In fact, when looked at in detail, the room-temperature EPR spectrum of the metHbA radical is similar to the five-component signal seen in the SW metMb and definitely different from the seven-component signal detected in HH metMb.

This paper will show for the first time a direct comparison between the EPR spectra seen at low temperature and room temperature after peroxide addition to Hb and Mb. This reveals that the nonperoxyl radical detectable as a singlet in the low-temperature EPR spectra is definitely caused by a tyrosine (Tyr) radical. The same species results in a five-component liquid-phase spectrum when studied at room temperature. The seven-component signal detectable in HH Mb arises from a different species.

MATERIALS AND METHODS

Protein purification

Human Hb samples were purified from a healthy donor's blood according to Antonini and Brunori (1971). The HH Mb (M-1882) and SW Mb type II (N.M.-0380; this product is no longer commercially available) were from Sigma Chemical Co. (St. Louis MO). Mutagenesis of the synthetic SW Mb gene (Springer and Sligar, 1987) was performed with the U.S.E. Mutagenesis Kit (Amersham Pharmacia, Uppsala, Sweden). The following oligonucleotide was used to mutate Tyr103 to Phe: 5′- CGCTTCAGAGAT**A**-AATTCCAGG**A**ATTTGATCGGG -3′; the nucleotide in bold indicates the mutation site. Screening of the mutants was carried out by restriction analysis, because the oligonucleotide deletes a unique *Eco*RI site (underlined character), and confirmed by sequencing the entire gene. Wild-type and mutant SW Mbs were expressed in *Escherichia coli* and purified to homogeneity as previously described (Cutruzzola et al., 1991). The expression levels of the Tyr103Phe mutant were comparable to that of the wild-type protein; no specific effect of the mutation on the protein yield was therefore observed as reported in (Wilks and Ortiz de Montellano, 1992). Because the starting gene used by these authors is different from the one used in this work (and the precise sequence was not published), a possible explanation may be found in a slightly different codon used to build the two wild-type genes and to design the Tyr103Phe mutagenic triplet.

H_2O_2 was purchased from Sigma-Aldrich Co. (Poole, UK). The protein samples were fully oxidized by addition of 2 mM ammonium persulfate and then passed down a Sephadex G-25 column. Oxidized stock solutions were diluted to 100 or 80 μM in 35 mM potassium phosphate buffer at different pH values. All buffers contained 20 μM DTPA (diethylenetriaminepentaacetic acid) as a free iron-chelating agent.

A Hewlett Packard 8453 diode array spectrophotometer was used for optical absorbance measurements. Final concentrations of protein preparations were measured using the ferrous CO complexes as standards. Aliquots of the oxidized proteins were reduced by addition of 10 mM dithionite and then bubbled with CO for 30 s. The following extinction coefficients for the CO-heme forms were used to calculate the heme concentrations (Antonini and Brunori, 1971): $\epsilon_{540} = 15.4$ $mM^{-1}cm^{-1}$ for HH Mb-CO, $\epsilon_{542} = 14.0$ mM^{-1} cm^{-1} for SW Mb-CO, and $\epsilon_{540} = 13.4$ mM^{-1} cm^{-1} for HbA-CO.

The final concentrations of the proteins in the met form were measured independently by EPR spectroscopy using the metHb and metMb standards, the concentrations of which were determined as reported earlier (Svistunenko et al., 2000). All quantitative EPR measurements were performed under nonsaturating conditions for all paramagnetic species (a microwave power of 0.05 mW and $T = 25$ K). The optical and EPR spectroscopy methods showed consistent results in protein determination with differences of less than 10%.

Control experiments with photosynthetic radicals

Arabidopsis thaliana (L.) variety Columbia seeds were germinated in general-purpose compost and grown at 24°C and 70% humidity at a light intensity of 180 μmol m^{-2} s^{-1} with a photoperiod of 16 h and 8 h of darkness in every 24-h cycle. Plants were grown until their rosettes were fully expanded, ~6 days before appearance of the flowering stalk. Plants were light-stressed at 2000 μmol m^{-2} s^{-1} for 1.5 h, and individual leaves were then detached at the petiole, inserted into EPR tubes, and frozen in liquid nitrogen until required.

Reaction of heme proteins with peroxide and EPR sampling

Low-temperature EPR experiments

A 1.2-ml aliquot of protein and a 50-μl aliquot of H_2O_2 were mixed and stirred using an electrical shaker. Wilmad SQ EPR tubes (Wilmad Glass, Buena, NJ) were used for EPR samples. To minimize the effect that slightly different size of the tubes might have on the quantitative results, only selected tubes were used with outer diameter 4.05 $\pm$ 0.07 mm and inner diameter 3.12 $\pm$ 0.04 mm (mean $\pm$ range). Tubes containing protein solutions or water (blank samples) were quickly frozen in methanol kept on dry ice. Once frozen, samples were transferred to liquid nitrogen (77 K) where they were stored before measurements. Storage of the samples in liquid nitrogen did not have any effect on the EPR spectra. When a set of samples was prepared by freezing aliquots of the same protein solution in the selected Wilmad SQ tubes, the random error in the EPR signal intensities observed in such samples was always very low (1–3%).

Room-temperature EPR experiments

A Wilmad WG-813-TMS Aqueous Cell (600-μl flat part and 800-μl upper tube) was used. A volume of 800 μl of protein was put in the cell, and a volume of 400 μl of H_2O_2 was added. A long syringe needle was used to inject solutions gently and close to the flat part of the cell, H_2O_2 being added directly to the protein solutions in the upper tube part. Immediately after addition of H_2O_2, the mixture was forced down the cell with a syringe attached with plastic tubing to the bottom of the aqueous cell. To ensure that the flat part of the cell was filled with the reaction mixture, the volume

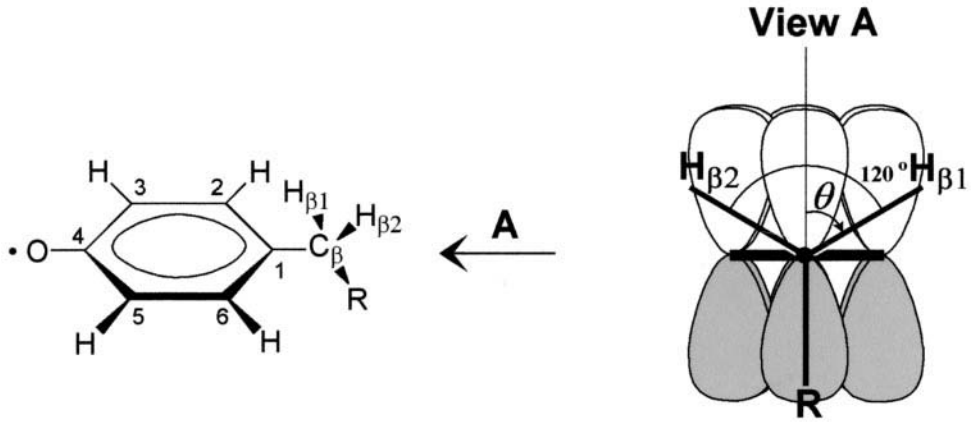

FIGURE 1 Definition of θ: the angle of the phenoxyl group rotation around C_1–C_β bond in tyrosine.

forced down the cell was 700 μl. We assumed that H_2O_2 was mixed with the protein solution in the upper tube part of the cell and did not have time to diffuse into the flat part. Therefore, the actual concentrations of the reactants in the liquid-phase experiments are only approximately known and indicated as targeted. The reproducibility of the experiments conducted with identical protocols was very good, so that the measured EPR spectra were completely superimposable.

EPR measurements and spectra processing

All EPR spectra were measured on a Bruker EMX EPR spectrometer (X-band) at a modulation frequency of 100 kHz. Accurate *g*-values were obtained using the built-in microwave frequency counter and a 2,2-diphenyl-1-picrylhydrazyl powder standard, the *g*-value for which is $g = 2.0037 \pm 0.0002$ (Weil et al., 1994). Other instrumental settings are in the figures and have the following abbreviations: microwave frequency ν (GHz), microwave power p (mW), modulation amplitude A_m (G), spectra sweep rate υ (G/s), time constant τ (ms), and number of scans per spectrum *NS*.

A spherical high quality Bruker resonator SP9703 and an Oxford Instruments liquid helium system were used to measure EPR spectra at low temperature. Unless stated otherwise, the EPR spectra were measured at 10 K. The EPR spectra of the blank samples (frozen water) were subtracted from the EPR spectra of the protein samples to eliminate the base line caused by the resonator's walls, quartz insert, or quartz EPR tube. The $g = 2$ component of the high spin met heme signal has been subtracted from the EPR spectra of the protein radicals. The first integrals of such corrected spectra converged over the integration range of 200 G in contrast to the spectra before subtraction of the $g = 2$ heme component, for which the integrals diverged.

Determination of the absolute concentration of the free radicals was performed using a set of Cu^{2+} concentration standards and double integration of the EPR pure lineshapes. The techniques of spectral subtraction with a variable coefficient (Svistunenko et al., 1996, 2000) were used to determine EPR signal intensities. Copper standards and protein samples were measured under nonsaturating conditions.

A 4103TM Bruker resonator was used in the room-temperature experiments. The EPR measurements were started 4–7 s after mixing, and the spectra were run consecutively in an automated regime without time delay between spectra. EPR spectra simulations were performed with WINEPR SimFonia 1.25 (Bruker Spectrospin Ltd., Coventry, UK). The EPR spectra of the SW metMb (Miki et al., 1989) and soybean metLb (Davies and Puppo, 1992) radicals were scanned and digitized with UN-SCAN-IT v.5.0 (Silk Scientific Corp., Orem, Utah).

Three-dimensional protein structure viewing

Swiss-PdbViewer v.3.5 was used to analyze the three-dimensional (3-D) structure of the proteins. Hydrogen atoms cannot be seen in the structures obtained from x-ray crystallography data, so the rotation angle θ in Tyr residues (see Fig. 1) cannot be measured directly. Instead, the tyrosine residue in question was oriented as shown in Fig. 1 to represent view A with C_β—R bond being below and not above the phenoxyl ring. We printed out the picture and measured with a protractor the angle ϕ formed by the C_β—R bond and the perpendicular to the phenoxyl ring (from the perpendicular drawn downwards, clockwise to the bond). The angle θ was than calculated as $\phi + 60^o$.

RESULTS

The type and the quantity of the radicals formed in metHb and metMb after addition of H_2O_2 is strongly dependent on the protein used. Fig. 2 shows the low-temperature EPR spectra of metHbA, SW metMb, and HH metMb before and 30 s after H_2O_2 addition. The anisotropic EPR signal with $g_\perp = 6$ and $g_\parallel = 2$ from the high-spin met form of heme (Fe^{III}) (Blumberg et al., 1968) decreases on H_2O_2 addition, indicating oxidation of the heme iron to the diamagnetic ferryl state Fe^{IV}═O. At the same time, a free radical is formed. Although the concentrations of the reactants and the pH values of the medium were the same in all three cases, the free radical EPR signal is different, by size and lineshape, in the three proteins. Two different EPR signals are present in all cases, the proportions of which vary between the proteins (Svistunenko, 2001). One of these two signals is the anisotropic spectrum of a peroxyl radical, with a parallel component at $g = 2.037$; this species is present at the highest concentration in the HH metMb spectrum. The other signal is an ~19-G wide singlet, present at highest concentration in the metHb spectrum. SW Mb differs only slightly in primary sequence from HH Mb so that the 3-D structures of the proteins are practically superimposable. This difference, however, results in a markedly different pattern of free radical formation. SW metMb responds to H_2O_2 like metHbA, not HH metMb, in that the singlet, and

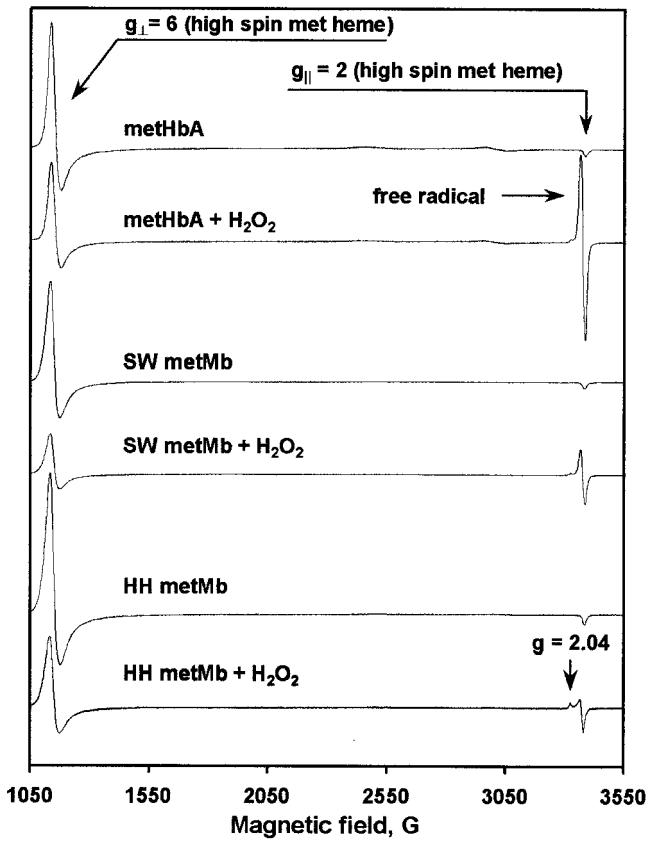

FIGURE 2 The EPR spectra of human metHb, SW metMb, and HH metMb before and 30 s after addition of H_2O_2. The 100 μM protein (by heme in the case of Hb) and 100 μM H_2O_2 were used in all three cases. The reaction was conducted at room temperature at pH 6. The EPR spectra were measured at 10 K. Other instrumental parameters were $\nu = 9.472$ GHz, $p = 0.8$ mW, $A_m = 4$ G, $\tau = 41$ ms, $\upsilon = 14.9$ G/s, and $NS = 1$.

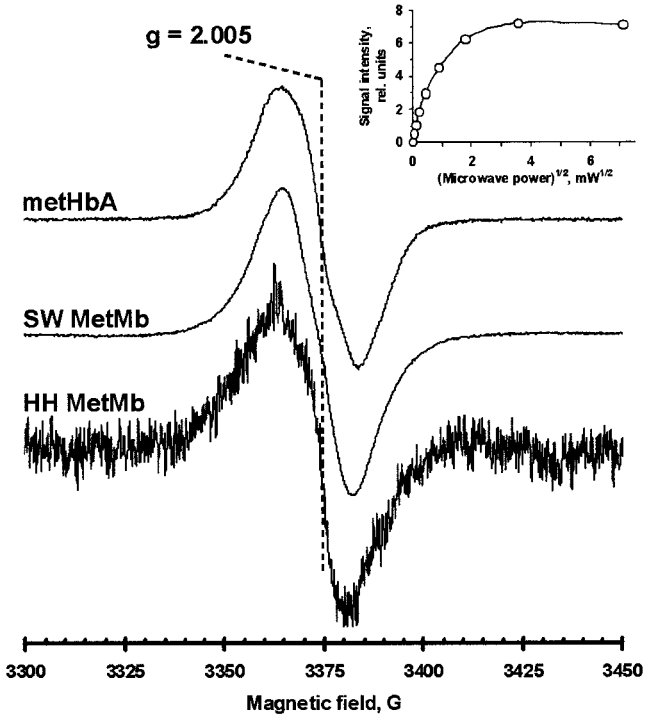

FIGURE 3 The singlet EPR signals detected in the spectra of metHbA, SW metMb, and HH metMb (100 μM by heme) mixed with equimolar amounts of H_2O_2. The signals shown are results of spectral subtraction procedures, designed individually in each case to attain the best (purest) singlet possible, after the original spectra were detected at optimal conditions for the subtraction procedure (see Appendix). The reaction was conducted at room temperature and pH 8 (metHbA) and pH 7.6 (SW metMb and HH metMb). The original spectra were measured at 10 K, $\nu = 9.468$ GHz, $A_m = 2$ G, $\tau = 41$ ms, and $\upsilon = 2.38$ G/s. Other instrumental conditions were $p = 0.8$ mW and $NS = 1$ (metHbA) or $p = 3.18$ mW and NS = 2 (SW metMb and HH metMb). The $g = 2$ component from the high-spin heme signal has been subtracted from all the spectra before applying the procedure of subtraction with variable coefficients. The intensity of all signals was normalized to the same peak-to-trough value. The inset shows the microwave power saturation curve for the singlet in metHbA.

not the peroxyl radical signal, dominates the EPR spectrum (Fig. 2). There is also a third kind of EPR signal that is present only in the HH metMb/H_2O_2 systems. This is a multicomponent signal seen in the low-temperature spectra at pH 6 and is probably due to the same species that is responsible for the seven-component signal in the liquid-phase spectra of the HH metMb/peroxide system (Miki et al., 1989).

Fig. 3 shows the pure lineshapes of the singlet in the three systems, obtained by the procedure of spectral subtraction with variable coefficients. The high level of noise in the HH Mb spectrum is an indication that the radical responsible for the singlet is formed at a low concentration in this protein under H_2O_2 treatment. The lineshape of the three singlets detected in metHbA, SW metMb, and HH metMb after addition of H_2O_2, are similar. Each is centered at $g = 2.005$ and has a peak-to-trough width of ~19 G. The microwave power saturation behavior of the signals is also similar. It is therefore likely that the free radicals responsible for the singlet EPR signal in the three proteins are located on analogous amino acid residues. Fig. 4 shows the kinetics of the radical formation and decay in metHbA, SW metMb, and HH metMb after addition of H_2O_2 at pH 7.6. The relative concentrations of the singlet (metHb > SW metMb > HH metMb) are maintained over the whole time course. We have reported before that the low, nonstoichiometric absolute concentration of the radicals often observed in such systems (Kelso King and Winfield, 1963; Kelso King et al., 1967) is a result of a pseudo-steady state, where the rates of radical formation and decay are both H_2O_2 concentration dependent (Svistunenko et al., 1997b). The lineshape of the singlet is essentially unchanged over the pH range 6–8 (illustrated for metHb in Fig. 5).

When the reaction of metHbA with H_2O_2 was studied at room temperature, a poorly resolved EPR signal was detected (Fig. 6). We have shown before, both at 10 K and at

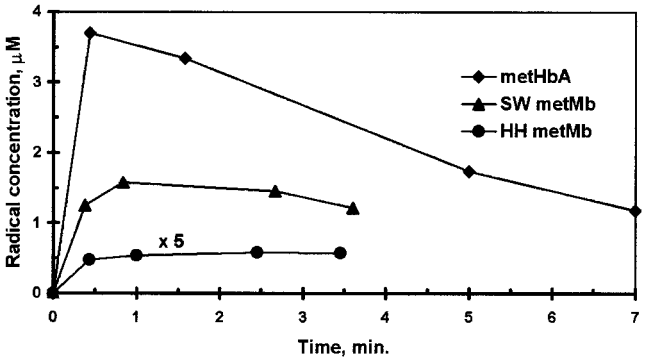

FIGURE 4 The kinetic dependences of the radicals with the singlet EPR signal in the three proteins after addition of H_2O_2. The proteins' concentrations (heme concentration in the case of Hb) and the concentration of H_2O_2 were 100 μM, pH 7.6. The radical concentrations for HH metMb were multiplied by 5 for illustrative purpose. The random error involved in the concentration measurements was 2–3%. The systematic errors associated with each series were estimated as $\pm$0.3 μM for metHbA, $\pm$0.4 μM for SW metMb, and $\pm$0.15 μM for HH metMb. The overall systematic error associated with the concentration axis was estimated as 20%.

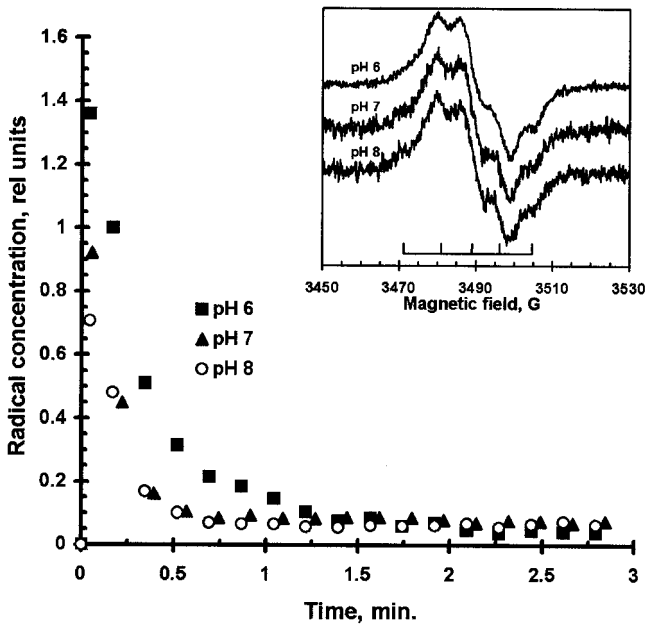

FIGURE 6 Kinetic dependences of the EPR signals detected at room temperature in 0.71 mM (heme) metHbA mixed with 7.1 mM H_2O_2 (targeted final concentrations) at three different pH values (aerated condition). The EPR spectra were measured in an automated consecutive manner at the following instrumental conditions: ν = 9.798 GHz, p = 1.27 mW, A_m = 2 G, τ = 10.2 ms, υ = 9.54 G/s (sweep time 10.5 sec), NS = 1, and T = 293 K. The spectra for the first time point of each dependence, normalized to equal amplitude, are shown in the inset. The data points correspond to the time of half-scan of each spectrum when the clock was started at the moment of mixing.

room temperature (Svistunenko et al., 1996, 1997b), that the free radical in the metHb/H_2O_2 system very rapidly reaches a steady state, the duration of which lengthens with increasing H_2O_2 molar excess. However, the steady-state radical concentration decreases with increasing molar ratio H_2O_2/heme (Svistunenko et al., 1996, 1997b). An experimentally optimal 10:1 ratio of H_2O_2 to heme was therefore used to observe the free radical for a longer duration. The EPR feature observed is best described as an anisotropic quintet; this signal is similar to that reported previously for this system (McArthur and Davies, 1993; Shiga and Imaizumi, 1975; Svistunenko et al., 1996). Fig. 6 shows the kinetic dependences of the signal at three different pH values. The signal decreases more rapidly at higher pH. The time taken to attain a steady state is twice as long at pH 6 as at pH 7 or 8, although the steady-state concentration is not strongly pH dependent. As is the case for the low-temperature singlet (Fig. 5), the lineshape of the five-component signal is similar in the pH range 6–8 (Fig. 6 *inset*). The lineshape does not change in the course of the reaction.

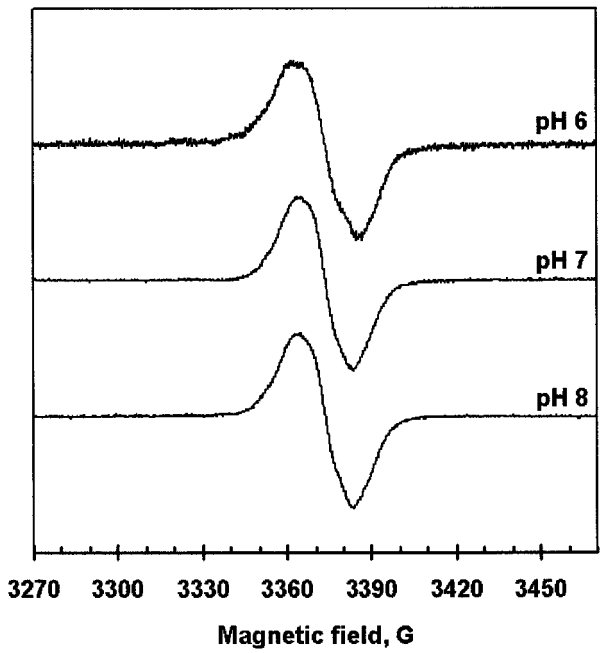

FIGURE 5 The singlet EPR signals detected at low temperature in the 100 μM metHbA/100 μM H_2O_2 systems at three different pH values. The spectra were obtained by using the procedure of spectral subtraction with variable coefficients as described in the Appendix. The original spectra were measured at 10 K, ν = 9.471 GHz, A_m = 2 G, τ = 41 ms, υ = 2.38 G/s, p = 0.8 mW, and NS = 1. The g = 2 component from the high-spin heme signal was subtracted from all spectra before applying the procedure of spectral subtraction.

The lineshape of the singlet detected in the frozen samples of the metHbA/H_2O_2 system (Fig. 5) is not completely featureless, suggesting an underlying hyperfine structure. We suggest that this singlet is caused by the same radicals as those responsible for the better-resolved liquid-phase spectrum (Fig. 6 *inset*) as the hyperfine structure seen at room temperature becomes less resolved when the sample is

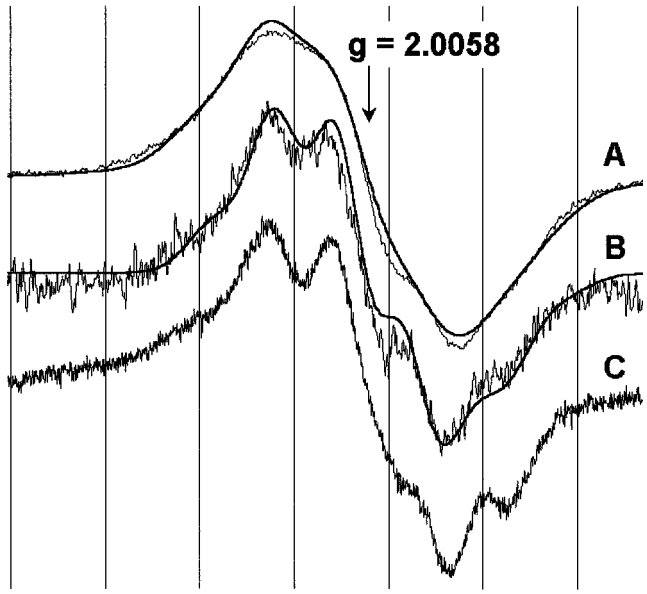

FIGURE 7 The EPR signals of the tyrosyl radical. (*A*) Spectrum of a frozen sample of 100 μM metHbA reacting with 100 μM H_2O_2 at pH 8. The sample was frozen 29 s after mixing, and the spectrum was measured at 10 K. Other instrumental parameters: $\nu = 9.471$ GHz, $p = 0.013$ mW, $A_m = 2$ G, $\tau = 41$ ms, $\upsilon = 2.38$ G/s, and $NS = 10$. (*B*) Spectrum measured at room temperature of metHbA reacting with H_2O_2 at pH 8 (the concentrations and instrumental parameters as in Fig. 6). A single scan was started 5 s after mixing and lasted for 10 s. (*C*) Difference spectrum ({whole leaves stressed by intense light for 1 h} − {whole unstressed leaves}); both stressed and control leaf spectra were measured at 10 K. Other instrumental conditions were $\nu = 9.473$ GHz, $p = 0.050$ mW, $A_m = 1$ G, $\tau = 82$ ms, $v = 0.42$ G/s, and $NS = 1$. The spectra were superimposed on the basis of the indicated *g*-factor, 2.0058. The noisy traces are the experimentally obtained spectra; the smooth traces overlaid with the experimental spectra *A* and *B* are the computer simulations with the parameters given in Table 1. The gridlines are drawn at a 10-G interval.

frozen. To check this we overlaid the spectra of the metHbA/H_2O_2 system measured at the same field width at room temperature and at 10 K (Fig. 7, *A* and *B*). Because microwave frequency differs between low-temperature and room-temperature EPR experiments, the resonance magnetic field for the same paramagnetic species is also different. The magnetic field axis is therefore omitted in Fig. 7, the signals being overlaid on the basis of their common *g*-factor. The hyperfine features discernible on the singlet fit well the five components of the liquid-phase spectrum (Fig. 7, *A* and *B*).

The liquid-phase spectrum can be simulated using the hyperfine splitting constants for a tyrosyl radical published previously (Fig. 7 *B* and Table 1). To attain the asymmetrical lineshape characteristic of the spectrum (Fig. 7 *B*), a *g*-factor anisotropy has to be introduced (Table 1). The 10 K spectrum of the singlet (Fig. 7 *A*) can then be simulated using a very similar set of parameters, merely requiring a slight increase of all hyperfine splitting constants and a slight decrease in the *g*-factor anisotropy (Table 1). The third spectrum in Fig. 7 *C* is shown for comparative purposes. It is the EPR signal of the radical produced in a green plant (*A. thaliana*) under high light stress. This spectrum has been well characterized as being due to a tyrosyl radical in photosystem II (Barry and Babcock, 1987; Barry et al., 1990; Warncke et al., 1994). The spectra in Fig. 7, *B* and *C*, are identical in lineshape.

Fig. 8 shows the EPR spectra of the wild-type recombinant SW metMb and of the Tyr103Phe variant, both proteins frozen 30 s after addition of an equimolar amount of H_2O_2 (spectra *a*). Both spectra *a* contain peroxyl radical signals, the features of which can be removed as described in the Appendix. The lineshape of the Trp peroxyl radical is slightly different in the wild type and the Tyr103Phe mutant, indicating that the symmetry of this radical in the mutant is more axial type than in the wild type. However, the integrated intensity of both signals, and hence concentration of the peroxyl radical, is similar in the two proteins (spectra *b*). In contrast, replacement of Tyr103 with a phenylalanine results in essentially a complete loss of the singlet EPR signal (spectra *c*).

DISCUSSION

In this study we have directly compared, for the first time, room- and low-temperature EPR spectra of the nonperoxyl radical formed after peroxide addition to ferric hemoglobin and myoglobin. We demonstrate that the singlet observed at low temperature is due to a tyrosine radical.

The first evidence that a tyrosine residue was involved in free radical formation after the reaction of heme proteins with peroxides was provided in Miki et al. (1989). Tetrani-

TABLE 1 Simulation parameters for the quintet of the tyrosyl radical in the metHbA/H_2O_2 system in the liquid and frozen states

	10 K (Fig. 7 *A*)	Room temperature (Fig. 7 *B*)
$a^H_{3,5}$, G	6.9	6.18 (DeGray et al., 1992; Sealy et al., 1985)
$a^H_{2,6}$, G	2.8	1.5 (Sealy et al., 1985)
$a^H_{\beta_1}$, G	7.1	6.7 (DeGray et al., 1992)
$a^H_{\beta_2}$, G	7.1	6.7 (DeGray et al., 1992)
$g_\parallel$	2.0028	2.001
$g_\perp$	2.0068	2.007
Line width, *G*	6.0	5.5
Lineshape	$L/G = 0.01$, almost Lorentzian	$L/G = 1$, pure Gaussian

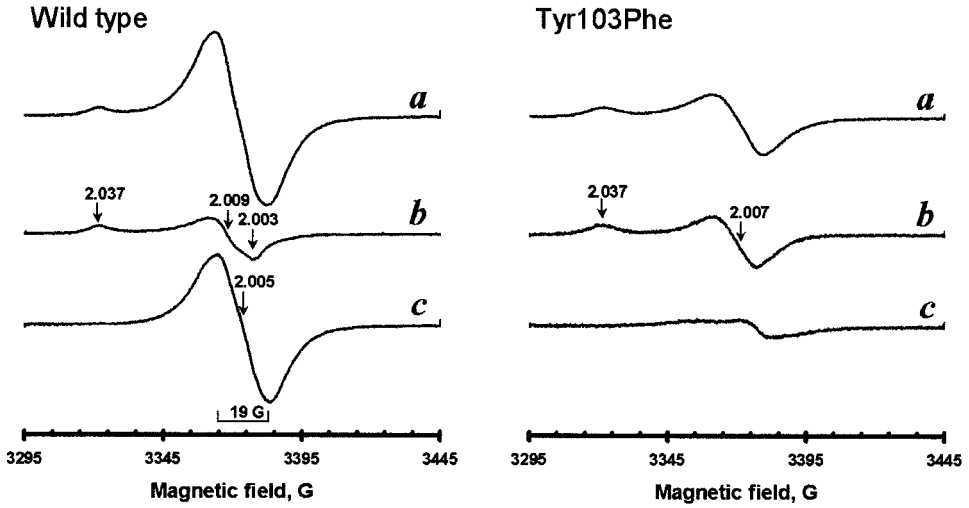

FIGURE 8 The EPR spectra of the wild-type recombinant SW metMb and the Tyr103Phe mutant. (*a*) Protein samples (80 μM) frozen 0.5 min after addition of H_2O_2 (80 μM) at pH 7; (*b*) Peroxyl radical signals pure lineshapes obtained as described in the Appendix; (*c*) Difference spectra $c = a - b$. The $g = 2$ component of the high-spin metMb has been subtracted from the experimental spectra, so that spectra *a* comprises only the free radical signals. The *g*-factors are indicated with arrows. Instrumental parameters were $\nu = 9.4681$ GHz, $p = 3.18$ mW, $A_m = 3$ G, $\tau = 164$ ms, $\upsilon = 0.89$ G/s, $NS = 1$, and $T = 10$ K.

tromethane treatment was used to remove only one Tyr from SW Mb, which treatment did not result in the loss of any tyrosines in HH Mb. The changes in the EPR spectra led the authors to suggest that the radical in SW metMb (with the five-component EPR signal) originated from Tyr151, the only one of the three SW Mb tyrosines not present in HH Mb (Miki et al., 1989).

Another five-component liquid-phase EPR signal, similar to that in the SW Mb/EtOOH system (Miki et al., 1989), was detected in soybean metleghemoglobin (metLb) immediately after mixing with H_2O_2 or other peroxides (Davies and Puppo, 1992). Lb, a monomeric oxygen-transporting heme protein in root nodules of legumes, is similar in sequence and structure to mammalian Mbs. However, there is no Tyr151 in Lb. Instead, there are three tyrosines at positions 25, 30, and 133 (Hargrove et al., 1997) (the last residue was identified as 132 in earlier studies (Fuchsman, 1985)). Davies and Puppo (1992) attributed the Lb radical to a tyrosine (possibly Tyr132/133) phenoxyl radical.

A five-component EPR signal is also detectable in the liquid phase in metHbA/peroxide systems. This signal, first reported for the metHb/H_2O_2 system in 1975 (Shiga and Imaizumi, 1975), was later shown for metHb reacting with other peroxides, such as EtOOH, 2-butanone peroxide, iodosylbenzene, or periodate (McArthur and Davies, 1993). When metHb was acetylated (to block tyrosine residues), the signal was not observed. The responsible species was therefore hypothesized to be a tyrosine phenoxyl radical (McArthur and Davies, 1993).

All these findings indirectly point to a possible link between the five-component spectrum and globin tyrosine residues. However, simulations of this signal in the past have not corresponded in detail to the lineshape of the experimental spectrum (McArthur and Davies, 1993). In this paper we show that the five-component signal in of metHbA is identical to the EPR spectrum of whole leaf (Fig. 7, *B* and *C*). The latter is known to originate from a tyrosyl radical of photosystem II (Barry and Babcock, 1987; Barry et al., 1990; Warncke et al., 1994). Furthermore, the five-component liquid-phase EPR signal in the metHbA/H_2O_2 systems can be simulated using the hyperfine splitting constants established for a tyrosyl radical elsewhere (Fig. 7 *B* and Table 1). The simulated and experimental spectra overlay precisely. Therefore, we have no doubt that the five-component EPR signal detected in the liquid phase of the metHb/peroxide system is due to a tyrosine radical.

Could it be that the other two five-component signals in SW Mb (Miki et al., 1989) and Lb (Davies and Puppo, 1992) are also caused by tyrosine radicals? These two signals have different lineshapes, each of which is also different from the Hb quintet. However, the overall widths of all three signals are similar. The SW metMb and metLb quintets can be simulated by hyperfine splitting constants that are characteristics of a tyrosine radical (Fig. 9). The major difference in the simulation parameters for the three globin radicals (Fig. 9 and Table 1) is the splitting constants on the methylene protons. Different splitting on the protons in different proteins can be explained by differences in the dihedral angles formed by the C_1-C_β-$H_{\beta 1}$ plane (or C_1-C_β-$H_{\beta 2}$) and the ring plane (Fig. 1).

As the phenoxyl ring rotates around the C_1—C_β bond, the spin density of the π-orbital system on the 1s orbitals of the methylene hydrogens (β-protons) changes according to a $\cos^2\theta$ pattern, where θ is the rotation angle (Stone and Maki, 1962). If θ is defined as shown in Fig. 1, then θ could be found from the following:

$$\begin{aligned} a^H_{\beta_1} &= \rho B'' \cos^2\theta \\ a^H_{\beta_2} &= \rho B'' \cos^2(\theta - 120^\circ), \end{aligned} \tag{2}$$

where $a^H_{\beta 1}$ and $a^H_{\beta 2}$ are experimentally measured hyperfine splitting constants on the two protons, ρ is spin density on C_1 and B'' is an empirical constant that defines β proton coupling constant $B = B' + B''\cos^2\theta$ (B' is negligible).

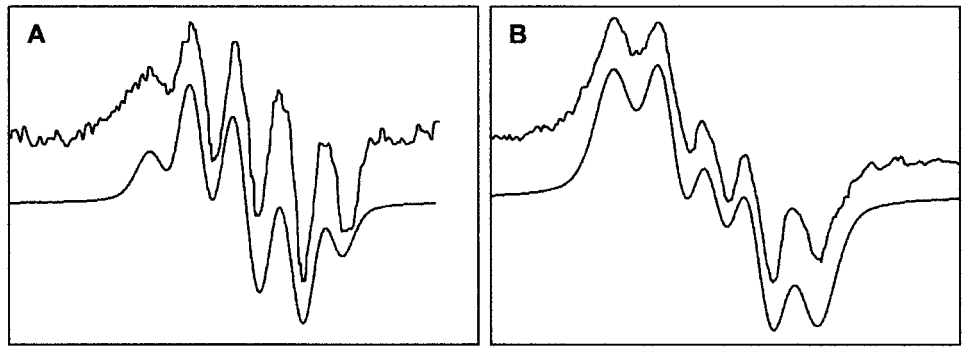

FIGURE 9 The EPR spectra assigned in the literature to Tyr radicals and our simulations of the spectra. (*A*) SW metMb/EtOOH (Miki et al., 1989) (*noisy trace*); this spectrum was simulated (*smooth trace*) for a Tyr radical (Fig. 1) with $g_{\perp} = 2.006$, $g_{\parallel} = 2.004$, $a^{H}_{3,5} = 5.2$ G, $a^{H}_{2,6} = 0$ G, $a^{H}_{\beta 1} = 8$ G, $a^{H}_{\beta 2} = 6.5$ G, and $\Delta H = 3.7$ G. (*B*) Soybean metLb/H_2O_2 (Davies and Puppo, 1992) (*noisy trace*); the parameters of the simulated spectrum were as follows: $g_{\perp} = 2.0046$, $g_{\parallel} = 2.0042$, $a^{H}_{3,5} = 6.4$ G, $a^{H}_{2,6} = 1.5$ G, $a^{H}_{\beta 1} = 12.5$ G, $a^{H}_{\beta 2} = 2.2$ G, and $\Delta H = 5.5$ G (*smooth trace*). Lorentzian lineshape was used in both simulations. Both *A* and *B* correspond to the 80-G field width increasing from left to right.

Thus, the hyperfine splitting constants on the two methylene protons follow the same $\cos^2\theta$ pattern but are phase-shifted with respect to each other by 120°, which is the angle between the C_β—H bonds.

System 3 was solved for the three sets of $a^{H}_{\beta 1}$ and $a^{H}_{\beta 2}$ presented in this paper for the Tyr radicals in the liquid phase in HbA, SW Mb, and soybean Lb (Table 1 and Fig. 9). Generally, Eq. 2 has four solutions on the θ range $-90°$ to $+90°$, two of which must be discarded as having a definitely wrong value for the second variable, $\rho B''$. The other two solutions are identical and indistinguishable as far as the EPR method is concerned. The sum of these two values of θ is strictly the angle between the two C_β—H bonds, i.e., 120° (Table 2).

Thus, the values of the methylene protons' hyperfine splitting constants, obtainable from the EPR spectrum of a Tyr radical, provide information about the dihedral angles in the radical and therefore indicate which Tyr residue in the protein could be the site of the radical. Sometimes the constants cannot be found precisely from an experimental EPR spectrum, for example, when one of the constants is smaller that the line width. This may limit the usefulness of this approach.

Angles θ found from Eq. 2 were compared with those determined from the 3-D structure (Table 2). It has been previously suggested that Tyr133 in Lb was the host of the free radical because it is the closest Tyr to the heme (Davies and Puppo, 1992). Our analysis confirms that the dihedral

TABLE 2 Rotation angle θ in the Tyr radical as determined from the hyperfine splitting constants on the methylene protons (Table 1 and Fig. 9) and as found for all tyrosines present in the proteins from the known 3-D structure

	EPR			X-ray analysis						
Protein	$a^{H}_{\beta_1}$	$a^{H}_{\beta_2}$	θ*	All tyrosines	Chain	$\theta^{\dagger}$	$\theta^{\dagger}$	Chain	$\theta^{\dagger}$	PDB file‡
HbA	6.7 G	6.7 G	**60°**	αTyr24	A	146°		C	138°	1HGB (Liddington et al., 1992)
				αTyr42	A	**63°**		C	**49°**	
				αTyr140	A	98°		C	98°	
				βTyr35	B	**52°**		D	**37°**	
				βTyr130	B	**50°**		D	**40°**	
				βTyr145	B	87°		D	85°	
SW Mb	8.0 G	6.5 G	58.3° or **61.7°**	Tyr103			134°			1A6K (Vojtechovsky et al., 1999)
				Tyr146			128°			
				Tyr151			**87°**			
Soybean Lb	12.5 G	2.2 G	**46.7°** or 73.3°	Tyr25	A	4°		B	15°	1BIN (Hargrove et al., 1997)
				Tyr30	A	30°		B	29°	
				Tyr133	A	**52°**		B	**52°**	

The closest values of θ identified by two different techniques are in bold; the corresponding Tyr residue (also in bold) is the main candidate for the site of the Tyr radical observed by EPR.

*Solutions of Eq. 2.

†Values found for specific Tyr residues from the 3-D structures as described in Materials and Methods.

‡Protein Data Bank (PDB) files are available from http://www.rcsb.org/pdb/. The 3-D structure was analyzed with the use of Swiss-Pdb Viewer 3.5 (http://tw.expasy.org/spdbv/).

angle in Tyr133 (52° as found from the protein's 3-D structure) is the closest to the angle derived from the radical's spectral features (46.7° as found from Eq. 2), and therefore Tyr133 is the most likely site responsible for the radical seen in Lb (Table 2). In SW Mb, Tyr151 seems the most likely candidate, because $\theta = 87°$ in this residue is closest to $\theta = 61.7°$ found as an Eq. 2 solution for the SW Mb EPR spectrum (Table 2). The situation is less clear in HbA, partly because the angles calculated from the x-ray structure vary for the same tyrosines in identical chains (A and C chains, α subunits; B and D, β subunits). However, αTyr42, βTyr35, and βTyr130 seem the most likely candidates (Table 2). As we will discuss later simple mutation of these residues is not likely to yield unequivocal data about where the radical resides in the wild-type protein. Therefore, more accurate information on the hyperfine splitting constants deducible from the EPR spectra and on the exact bond angles in the protein structure are equally important for final assignment of the radical to a specific residue.

The low-temperature EPR of globin radicals has also been extensively studied. How can the low-temperature EPR signals be related to those observed at room temperature? The EPR spectra of the HH metMb/H_2O_2 system measured at a low temperature show mainly a peroxyl radical. This cannot be formed from a tyrosine radical and was demonstrated to originate from a tryptophan residue (DeGray et al., 1997; Gunther et al., 1995). Similar peroxyl radicals are also present in the frozen metHbA/H_2O_2 system. However, the major feature in these spectra is a singlet EPR signal. The SW metMb/H_2O_2 system is in an intermediate situation with the peroxyl radical and singlet signals both contributing strongly to the spectrum (Fig. 2).

When looked at in detail, the low-temperature singlet in metHbA has an underlying hyperfine structure (Fig. 7 *A*). When overlaid with the liquid-phase spectrum, it becomes clear that the features on the lineshape of the singlet correspond well to the components of the liquid-phase quintet. The singlet could be simulated with parameters only slightly different from those used to simulate the liquid-phase tyrosine radical spectrum (Fig. 7 and Table 1). We conclude therefore that the singlet EPR signal observed at low temperature in the metHbA/H_2O_2 system is caused by a tyrosine radical. Room-temperature EPR has not been able to detect directly free radicals in blood. However, a signal is seen at low temperature. This signal is identical to that produced after peroxide addition to metHb in vitro (Svistunenko et al., 1997a,b). Therefore, we now can state unequivocally that the identity of the free radical seen in frozen blood is a hemoglobin-bound tyrosine radical.

Because the parameters and properties of the singlets are similar in the three globins studied (Figs. 2 and 3), it is likely that tyrosyl radicals are responsible in each case. When the three proteins are compared, a correlation can be seen between the intensities of the liquid-phase quintet (definitively assigned to tyrosine) and the 10 K singlet. The strongest singlet and the strongest quintet are both seen in HbA. The singlet is smaller in SW Mb and much smaller in HH metMb (Fig. 4). This is in accordance with the result that the liquid-phase quintet was detected in the SW metMb/peroxide system but was not seen in the HH metMb under similar conditions (Miki et al., 1989). We therefore suggest that the singlet EPR signals observed at low temperature in SW metMb and HH metMb under H_2O_2 treatment (Fig. 3) are also caused by tyrosyl radicals.

All possible Tyr-to-Phe mutants of recombinant SW metMb were studied in their reaction with H_2O_2 (Wilks and Ortiz de Montellano, 1992). However, in this study, there was a significant contribution from a peroxyl radical signal in all spectra. Not subtracting the contribution of this species from the overall spectra made comparisons between the Tyr mutants difficult. We have undertaken a similar study of the Tyr103Phe mutant. We show that, after subtraction of the signal from the (tryptophan) peroxyl radical the Tyr103Phe mutant has essentially no singlet signal: changing Tyr103 to Phe has completely removed the tyrosine radical. Yet our spectral analysis (Table 2) suggests that Tyr103 is not in the correct conformation to explain the hyperfine constants of the Tyr radical observed in the liquid phase: θ in Tyr103 is 134° as can be found from the 3-D structure, whereas the EPR spectrum (quintet in Fig. 9 *A*) suggests that $\theta = 58.3°$ or $\theta = 61.7°$ (the two solutions of Eq. 2 with $a^H_{\beta 1} = 8.0$ G and $a^H_{\beta 2} = 6.5$ G as parameters). Instead, Tyr151 ($\theta = 87°$) is a more likely candidate. Interestingly, the Tyr151Phe mutant also seems to show a diminished singlet signal, just like the Tyr103Phe mutant (Wilks and Ortiz de Montellano, 1992). Tyr103 is the closest to the heme. We suggest the radical forms first on Tyr103; a rapid electron transfer between this primary site and Tyr151 then occurs. Tyr151 is the more stable radical detectable in the steady state. Mutations in either Tyr103 or Tyr151 can therefore block the formation of a significant Tyr free radical signal in SW Mb. The fact that both Tyr103 and Tyr151 free radicals can be spin trapped in SW metMb reacting with H_2O_2 (Gunther et al., 1998) is consistent with such a mechanism.

APPENDIX

Pure lineshapes of the singlet EPR signal in the three proteins (Fig. 3)

The singlet EPR signals shown in Fig. 3 were obtained by the procedure of spectral subtraction with the variable coefficients outlined below.

The EPR spectra are shown in brackets. The brackets with time values correspond to the EPR spectra of the protein frozen at the indicated time after addition of H_2O_2. The coefficients of subtraction were varied; those indicated below are the best to eliminate the peroxyl radical EPR signal (and other minor signals):

$$\{\text{MetHbA}\} = \{0.48\ \text{min}\} - 0.58\{1.67\ \text{min}\}.$$

$$\{\text{SW metMb}\} = \{2.67\ \text{min}\} - 0.14\ \{\text{A}\}.$$

Spectrum A represents the pure lineshape of the peroxyl radical spectrum, obtained as follows:

$$\{A\} = \{0.38\ \text{min}\} - 0.75\ \{0.83\ \text{min}\}$$

$$\{\text{HH metMb}\} = \{B\} - 0.10\ \{C\}.$$

Spectrum B represents the singlet superimposed with a low-intensity peroxyl radical signal:

$$\{B\} = \{3.45\ \text{min}\} - 0.32\ \{2.45\ \text{min}\}.$$

Spectrum C is the pure lineshape peroxyl radical signal:

$$\{C\} = \{0.43\ \text{min}\} - 0.76\ \{1\ \text{min}\}.$$

Pure lineshapes of the singlet EPR signal in metHb at different pH values (Fig. 5)

The reaction between 100 μM metHbA (heme concentration) and 100 μM H_2O_2 was conducted at room temperature at pH 6, 7, and 8. The samples of the reaction mixture were frozen at the time indicated in brackets. The procedures of spectral subtraction were as follows.

The singlet at pH 6 was obtained as {5.00 min} − 1.20{D}, where {D} = {1.50 min} − 0.48{0.43 min}. Spectrum D is a broad signal of low intensity that is left when the peroxyl radical signal is eliminated (this happens when the coefficient of subtraction equals 0.48). This broad signal arises from an unidentified minor species.

The singlet at pH 7 was obtained as {1.50 min} − 1.04{5.00 min}.

The singlet at pH 8 was obtained as {0.48 min} − 0.56{1.67 min}.

Pure lineshapes of the peroxyl radical EPR signals in SW metMb (Fig. 8 *b*)

The peroxyl radical EPR signals (Fig. 8 *b*) were obtained by the procedure of spectral subtraction with variable coefficients. The samples of wild-type recombinant SW metMb and the Tyr103Phe variant (both at 80 μM, pH 6–8) were frozen at various times elapsed from the addition of equimolar amount of H_2O_2. The primary EPR spectra were measured at the instrumental conditions indicated in the Fig. 8 legend. The $g = 2$ component from the high-spin heme signal had been subtracted from all spectra before applying the procedure of subtraction with variable coefficients. These procedures for the two proteins are outlined below (the EPR spectra are given in brackets). The times elapsed after addition of H_2O_2 and the pH value at which the reaction was conducted are indicated in the brackets.

In the wild-type (wt) protein, the pure lineshape peroxyl radical spectrum (Fig. 8 *b* on the left) was obtained as follows: $\{b\}_{wt} = 0.41 \times \{[(\{0.50\ \text{min; pH 8}\} - 0.77 \times \{1.07\ \text{min; pH 8}\}) + (\{0.50\ \text{min; pH 8}\} - 0.70 \times \{1.67\ \text{min; pH 8}\}) + (\{1.07\ \text{min; pH 8}\} - 1.08 \times \{2.88\ \text{min; pH 8}\})] - 0.66 \times [(\{0.72\ \text{min; pH 6}\} - 1.11 \times \{1.73\ \text{min; pH 6}\}) + (\{0.72\ \text{min; pH 6}\} - 1.00 \times \{1.25\ \text{min; pH 6}\})]\}$.

The logic behind these expressions is as follows. The singlet EPR signal was eliminated in the three difference spectra for pH 8, and these three spectra were then averaged by summing up. Similarly, two difference spectra for pH 6 were constructed and averaged. The resultant two spectra contain the peroxyl radical signal as the main component (because the singlet has been eliminated); the other, minor, spectral components are at different levels at pH 8 and pH 6. These minor components were eliminated in the new difference spectrum when the averaged spectrum at pH 6 was multiplied by 0.66 and subtracted from the averaged spectrum at pH 8. Finally, the result was multiplied by 0.41 to make the peroxyl radical signal's intensity exactly as it is in the wild type's spectrum *a* in Fig. 8.

In the Tyr103Phe variant protein, the pure lineshape peroxyl radical spectrum (Fig. 8 *b* on the right) was obtained as an average of three difference spectra constructed from the pH 8 group, in which the minor, nonperoxyl radical spectral components were eliminated. The resultant averaged was multiplied by 2.66 to make the intensity of the peroxyl radical exactly as it is in the mutant's spectrum *a* in Fig. 8: $\{b\}_{Tyr103Phe} = 2.66 \times [(\{1.00\ \text{min; pH 8}\} - 0.98 \times \{1.67\ \text{min; pH 8}\}) + (\{1.00\ \text{min; pH 8}\} - 1.14 \times \{2.98\ \text{min; pH 8}\}) + (\{1.67\ \text{min; pH 8}\} - 1.23 \times \{4.20\ \text{min; pH 8}\})]$.

We acknowledge the technical assistance of Neil Barnard.

This work was supported by the Wellcome Trust (D.S. and B.R.) and Biotechnology and Biological Sciences Research Council (M.F. and J.D.).

REFERENCES

Antonini, E., and M. Brunori. 1971. Hemoglobin and myoglobin in their reactions with ligands. Frontiers of Biology. North-Holland, Amsterdam.

Barry, B. A., and G. T. Babcock. 1987. Tyrosine radicals are involved in the photosynthetic oxygen-evolving system. *Proc. Natl. Acad. Sci. U.S.A.* 84:7099–7103.

Barry, B. A., M. K. el-Deeb, P. O. Sandusky, and G. T. Babcock. 1990. Tyrosine radicals in photosystem II and related model compounds: characterization by isotopic labeling and EPR spectroscopy. *J. Biol. Chem.* 265:20139–20146.

Blumberg, W. E., J. Peisach, B. A. Wittenberg, and J. B. Wittenberg. 1968. The Electron structure of protoheme proteins. I. An electron paramagnetic resonance and optical study of horseradish peroxidase and its derivatives. *J. Biol. Chem.* 243:1854–1862.

Burgova, E. N., A. F. Vanin, E. A. Demurov, and I. V. Proshina. 1989. Effect of the hyperbaric oxygenation of animals and man on mitochondrial function in their tissues (based on EPR study data). *Izv. Akad. Nauk SSSR Ser. Biol.* 2:191–197.

Chernov, G. A., T. G. Shlyakova, V. L. Sharygin, V. G. Sharf, I. N. Todorov, Y. I. Mitrokhin, O. I. Efremova, D. S. Khristianovich, T. V. Rozantseva, and M. K. Pulatova. 1994. The molecular aspects of the action of the radioprotector indralin. *Izv. Akad. Nauk SSSR Ser. Biol.* 1:20–37.

Cutruzzola, F., C. T. Allocatelli, P. Ascenzi, M. Bolognesi, S. G. Sligar, and M. Brunori. 1991. Control and recognition of anionic ligands in myoglobin. *FEBS Lett.* 282:281–284.

Davies, M. J., and A. Puppo. 1992. Direct detection of a globin-derived radical in leghemoglobin treated with peroxides. *Biochem. J.* 281: 197–201.

DeGray, J. A., M. R. Gunther, R. Tschirret-Guth, P. R. Ortiz de Montellano, and R. P. Mason. 1997. Peroxidation of a specific tryptophan of metmyoglobin by hydrogen peroxide. *J. Biol. Chem.* 272:2359–2362.

DeGray, J. A., G. Lassmann, J. F. Curtis, T. A. Kennedy, L. J. Marnett, T. E. Eling, and R. P. Mason. 1992. Spectral analysis of the protein-derived tyrosyl radicals from prostaglandin H synthase. *J. Biol. Chem.* 267:23583–23588.

Fuchsman, W. H. 1985. Discrepancies among published amino acid sequences of soybean leghemoglobins: experimental evidence against cultivar differences as the sources of the discrepancies. *Arch. Biochem. Biophys.* 243:454–460.

Gibson, J. F., and D. J. E. Ingram. 1956. Location of free electrons in porphin ring complexes. *Nature.* 178:871–872.

Gibson, J. F., D. J. E. Ingram, and P. Nicholls. 1958. Free radical produced in the reaction of metmyoglobin with hydrogen peroxide. *Nature.* 181: 1398–1399.

Gunther, M. R., D. J. Kelman, J. T. Corbett, and R. P. Mason. 1995. Self-peroxidation of metmyoglobin results in formation of an oxygen-reactive tryptophan-centered radical. *J. Biol. Chem.* 270:16075–16081.

Gunther, M. R., R. A. Tschirret-Guth, H. E. Witkowska, Y. C. Fann, D. P. Barr, P. R. Ortiz de Montellano, and R. P. Mason. 1998. Site-specific spin trapping of tyrosine radicals in the oxidation of metmyoglobin by hydrogen peroxide. *Biochem. J.* 330:1293–1299.

Hargrove, M. S., J. K. Barry, E. A. Brucker, M. B. Berry, G. N. Phillips, Jr., J. S. Olson, R. Arredondo-Peter, J. M. Dean, R. V. Klucas, and G. Sarath. 1997. Characterization of recombinant soybean leghemoglobin a and apolar distal histidine mutants. *J. Mol. Biol.* 266:1032–1042.

Kelso King, N., F. D. Looney, and M. E. Winfield. 1967. Amino acid free radicals in oxidised metmyoglobin. *Biochim. Biophys. Acta.* 133:65–82.

Kelso King, N., and M. E. Winfield. 1963. The mechanism of metmyoglobin oxidation. *J. Biol. Chem.* 238:1520–1528.

Liddington, R., Z. Derewenda, E. Dodson, R. Hubbard, and G. Dodson. 1992. High resolution crystal structures and comparisons of T state deoxyhaemoglobin and two liganded T-state haemoglobins: T(a-oxy)haemoglobin and T(met)haemoglobin. *J. Mol. Biol.* 228:551–579.

McArthur, K. M., and M. J. Davies. 1993. Detection and reactions of the globin radical in haemoglobin. *Biochim. Biophys. Acta.* 1202:173–181.

Miki, H., K. Harada, I. Yamazaki, M. Tamura, and H. Watanabe. 1989. Electron-spin resonance-spectrum of Tyr-151 free-radical formed in reactions of sperm whale metmyoglobin with ethyl hydroperoxide and potassium irridate. *Arch. Biochem. Biophys.* 275:354–362.

Pulatova, M. K., G. T. Rikhireva, and Z. V. Kuropteva. 1989. Electron Paramagnetic Resonance in Molecular Radiobiology. Energoatomizdat, Moscow.

Sealy, R. C., L. Harman, P. R. West, and R. P. Mason. 1985. The electron-spin resonance-spectrum of the tyrosyl radical. *J. Am. Chem. Soc.* 107:3401–3406.

Shiga, T., and K. Imaizumi. 1975. Electron spin resonance study on peroxidase- and oxidase-reactions of horseradish peroxidase and methemoglobin. *Arch. Biochem. Biophys.* 167:469–479.

Springer, B. A., and S. G. Sligar. 1987. High-level expression of sperm whale myoglobin in *Escherichia coli. Proc. Natl. Acad. Sci. U.S.A.* 84:8961–8965.

Stone, E. W., and A. H. Maki. 1962. Hindered internal rotation and ESR spectroscopy. *J. Chem. Phys.* 37:1326–1333.

Svistunenko, D. A. 2001. An EPR study of the peroxyl radicals induced by hydrogen peroxide in the heme proteins. *Biochim. Biophys. Acta.* 1546: 365–378.

Svistunenko, D. A., N. A. Davies, M. T. Wilson, R. P. Stidwill, M. Singer, and C. E. Cooper. 1997a. Free radical in blood: a measure of haemoglobin autoxidation in vivo? *J. Chem. Soc. Perkin Trans.* 2:2539–2543.

Svistunenko, D. A., R. P. Patel, S. V. Voloshchenko, and M. T. Wilson. 1997b. The globin-based free radical of ferryl hemoglobin is detected in normal human blood. *J. Biol. Chem.* 272:7114–7121.

Svistunenko, D. A., R. P. Patel, and M. T. Wilson. 1996. An EPR investigation of human methaemoglobin oxidation by hydrogen peroxide: methods to quantify all paramagnetic species observed in the reaction. *Free Radic. Res.* 24:269–280.

Svistunenko, D. A., M. A. Sharpe, P. Nicholls, M. T. Wilson, and C. E. Cooper. 2000. A new method for quantitation of spin concentration by EPR spectroscopy: application to methemoglobin and metmyoglobin. *J. Magn. Reson.* 142:266–275.

Vithayathil, A. J., J. L. Ternberg, and B. Commoner. 1965. Changes in electron spin resonance signals of rat liver during chemical carcinogenesis. *Nature.* 207:1246–1249.

Vojtechovsky, J., K. Chu, J. Berendzen, R. M. Sweet, and I. Schlichting. 1999. Crystal structures of myoglobin-ligand complexes at near-atomic resolution. *Biophys. J.* 77:2153–2174.

Warncke, K., G. T. Babcock, and J. McCracken. 1994. Structure of the Y-D tyrosine radical in photosystem-II as revealed by H-2 electron-spin echo envelope modulation (ESEEM) spectroscopic analysis of hydrogen hyperfine interactions. *J. Am. Chem. Soc.* 116:7332–7340.

Weil, J. A., J. R. Bolton, and J. E. Wertz. 1994. Electron Paramagnetic Resonance: Elementary Theory and Practical Applications. Wiley, New York. 511.

Wilks, A., and P. R. Ortiz de Montellano. 1992. Intramolecular translocation of the protein radical formed in the reaction of recombinant sperm whale myoglobin with H_2O_2. *J. Biol. Chem.* 267:8827–8833.